Thermochimica Acta, 186 (1991) 131–143
Elsevier Science Publishers B.V., Amsterdam

Study of the eutectic and monotectic of the acenaphthene–succinonitrile system

U.S. Rai and H. Shekhar

Department of Chemistry, Banaras Hindu University, Varanasi-221 005 (U.P.) (India)

(Received 17 December 1990)

Abstract

The solid–liquid equilibrium data on a faceted–non-faceted system involving acenaphthene and succinonitrile show the formation of a eutectic (0.99 mole fraction of succinonitrile) and a monotectic (0.35 mole fraction of succinonitrile) with a liquid miscibility gap in the system. From a study of solidification behaviour of the pure components, the eutectic and the monotectic, by measuring the growth rate of the moving front in a capillary, it can be inferred that the solidification rate of the monotectic is higher than that of the eutectic, and that the latter solidifies by the alternate nucleation mechanism. Using heats of fusion data, the entropies of fusion, the excess thermodynamic functions, the interfacial energies and the radius of critical nucleus at different degrees of undercooling were calculated and the validity of Cahn's wetting condition for the system was justified. A plausible explanation was given for the cellular dendritic morphology of the eutectic and a regular array of succinonitrile droplets in the microstructure of the monotectic.

INTRODUCTION

It is well known that the development of new materials with high strength, rigidity and ductility at high temperature has become a demand of the modern age of science. During the past two decades there has been immense interest in the fundamental understanding of solidification [1,2] and properties of polyphase alloys, and in the technological development of in situ composites for various applications. These materials are of remarkable commercial and technical importance because of the unusual anisotropic properties that result from their aligned microstructure. Although metallic [3–5] eutectics, monotectics and intermetallic compounds constitute an interesting area of investigation in metallurgy and materials science, they are not suitable for a detailed study of the parameters which control the mechanism of solidification, such as high transformation temperature, opacity, convection effects and limited choice of material present serious problems. Direct observation of the solidification interface of transparent organic systems [6–10] has been the most useful technique for unravelling the mysteries of solidification.

0040-6031/91/$03.50

A monotectic reaction [11] is characterised by the breakdown of a liquid phase into one solid and one liquid phase. In many respects this phase transformation resembles eutectic freezing, which involves isothermal decomposition of one liquid phase into two solid phases. However, less attention has been focussed on the study of monotectic alloys because of the limited choice of materials and the more extensive experimental difficulties associated with the miscibility gap. Because of their low transformation temperature, ease of purification, transparency and lack of convection, and the wider choice of materials, organic systems offer a simple and convenient method for a detailed physicochemical study of monotectic reactions. Acenaphthene (ACN) is a material of high enthalpy of fusion, which simulates non-metallic solidification and succinonitrile (SCN), with low entropy of fusion, solidifies like a metal. As such, the SCN–ACN system may be chosen as a suitable analogue of the Al–Si or Fe–C (metal–non-metal) system for direct observation on solidification. Recently there have been several articles [12–14] explaining the various interesting phenomena during the solidification of a monotectic alloy; particularly, the role of wetting in a phase-separation process has been a subject of great discussion. With a view to studying the chemistry of the organic eutectic and monotectic with a particular interest in the role of interfacial energy in their solidification, the ACN–SCN system has been chosen, and its phase diagram, growth kinetics, thermochemistry and microstructure have been studied.

EXPERIMENTAL

Materials and purification

Succinonitrile (Aldrich, Germany) was purified by repeated distillation under vacuum. Acenaphthene (Fluka, Switzerland) was recrystallised from boiling ethanol. The purity of each compound was checked by determining its melting point, which showed good agreement with the literature value.

Phase diagram study

The phase diagram of the ACN–SCN system was determined by the thaw–melt method. The experimental details have already been described in earlier communications [15,16].

Growth kinetics

The linear velocity of crystallisation of pure components, eutectic and monotectic was studied by determining the rate of movement of the growth front in a capillary. The experimental details were reported earlier [17,18].

Thermochemistry

Heats of fusion of the pure components and the eutectic were determined [19,20] by the DTA method.

Microstructure

Microstructures of the parent components, the eutectic and the monotectic were recorded [21,22] using an optical microscope (Leitz Laborlux D) attached to a camera.

RESULTS AND DISCUSSION

Phase diagram

The phase diagram of the ACN–SCN system (Fig. 1) shows the formation of a monotectic (0.35 mole fraction of SCN) and a eutectic (0.99 mole fraction of SCN). The eutectic and the monotectic temperatures correspond to 49.5 °C and 87.0 °C, respectively. Above a critical temperature (T_c) the two components are miscible in all proportions. Below this temperature, and between certain composition limits indicated by $L_1 + L_2$ in the figure, two immiscible liquids are produced. When a liquid of monotectic composition (M) is cooled through the monotectic horizontal (T_M), the monotectic reaction occurs, and a liquid L_1 which is rich in ACN decomposes into a

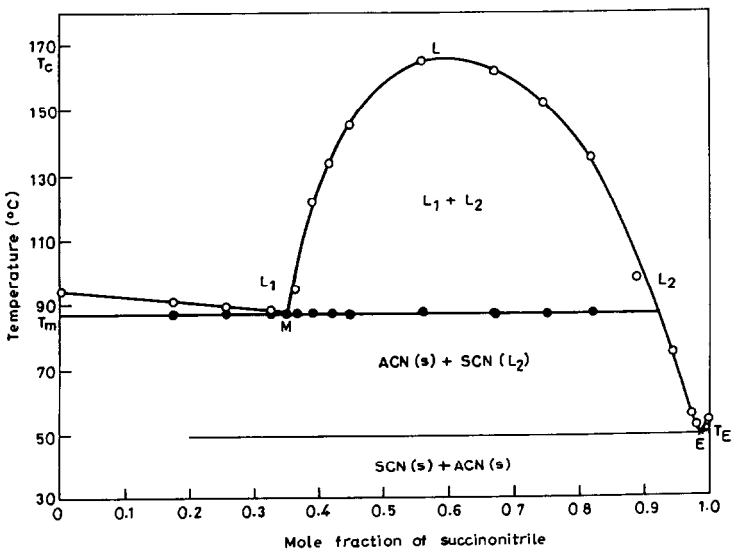

Fig. 1. Phase diagram of acenaphthene–succinonitrile system. (○) Melting temperature; (●) thaw temperature.

solid phase rich in ACN and another liquid phase L_2 (rich in SCN). At the monotectic temperature this reaction can be shown as

$$L_1 \rightleftharpoons S + L_2$$

$$L_1 \text{ (rich in ACN)} \rightleftharpoons \text{ACN(S)} + L_2 \text{ (rich in SCN)}$$

When a liquid of eutectic composition is allowed to cool below the eutectic horizontal T_E, a eutectic reaction takes place and the eutectic liquid decomposes into two solids. At the eutectic temperature this reaction can be shown as

$$L_2 \rightleftharpoons S_1 + S_2$$

$$L_2 \text{ (rich in SCN)} \rightleftharpoons S_1 \text{ (ACN)} + S_2 \text{ (SCN)}$$

Thus, the monotectic reaction is similar to the eutectic reaction except that one of the product phases of the monotectic reaction is a second liquid phase. The melting points of SCN and ACN are 54.0 °C and 94.0 °C, respectively. The critical solution temperature (165.0 °C) is 78.0 °C above the monotectic horizontal indicated by T_M (87.0 °C).

Growth kinetics

The eutectic solidification is a well known phenomenon verified by many experiments. On the other hand, only a limited number of experiments have been performed on monotectic systems and no general theory has been developed. However, Derby and Favier [23] have extended the Jackson–Hunt theory [9] on eutectics to monotectics as well. In the present system, acenaphthene is a high entropy of fusion component and it will solidify with faceted growth in a definite crystallographic orientation. Conversely, succinonitrile is a low entropy of fusion material and it will solidify with non-faceted morphology having no specific orientation. The final growth morphology will be decided by the interplay between the growth rate, the temperature gradient adjacent to the interface and the diffusion coefficient of the component phases at the interface. When the monotectic is cooled, ACN (for which the kinetic undercooling is very large) nucleates first, and the final morphology will be decided by the wetting behaviour of the phases involved.

The linear velocity of crystallization (v) of pure components, eutectic and monotectic was studied at different undercoolings (ΔT) and the data are expressed in the form of log v vs. log ΔT plots (Fig. 2). A linear dependence of these plots for all the materials in the system under investigation suggests the applicability of the Hillig–Turnbull equation [24]

$$v = u(\Delta T)^n \tag{1}$$

where u and n are constants depending on the solidification behaviour of the phases involved. The values of u and n were calculated from the linear

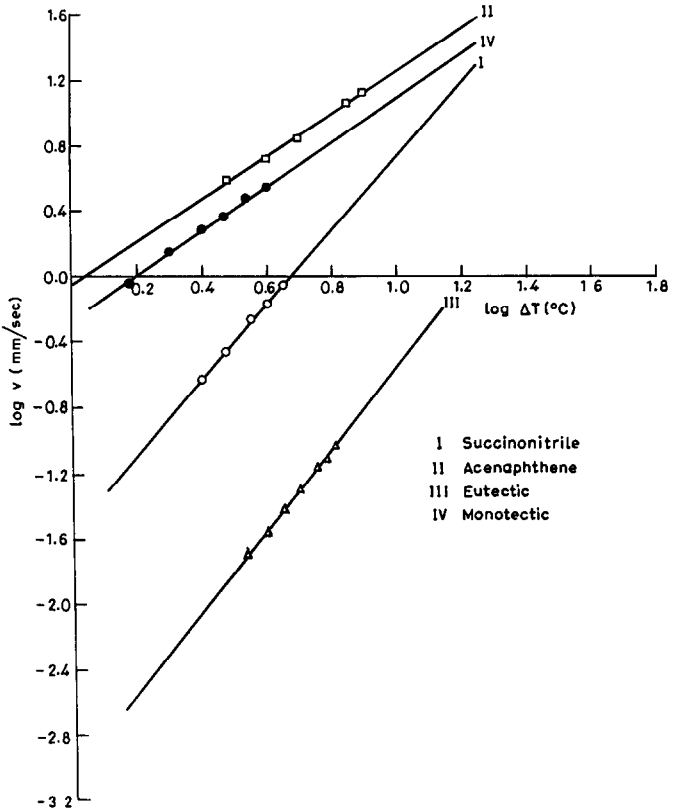

Fig. 2. Linear velocity of crystallisation of parent components, eutectic and monotectic.

plots and the results are reported in Table 1. It is evident that the values of n are close to 2, thereby suggesting a square relationship between the growth velocity and the undercooling. The deviations [15] of n from 2 observed in some cases may be due to differences in bath and interface temperatures. The values of the constant u, which gives a measure of the rate of solidification of a material, are also presented in Table 1. It is evident from the table that the growth rate of the monotectic is much higher than that of

TABLE 1

Values of u and n for pure components, eutectic and monotectic

Material	u (mm s^{-1} deg^{-1})	n
Acenaphthene	9.333×10^{-1}	1.30
Succinonitrile	2.917×10^{-2}	2.27
ACN–SCN eutectic	9.772×10^{-4}	2.51
ACN–SCN monotectic	5.310×10^{-1}	1.35

the eutectic at a particular undercooling. This may be due to the higher diffusion rate of the components in the liquid phase present in the monotectic. A similar conclusion was drawn in the case of the phenanthrene–succinonitrile system reported elsewhere [11]. It is also clear from the table that the growth velocity of the eutectic is smaller than those of the pure components. This may be explained in the light of the mechanism proposed by Winegard et al. [25]. From this mechanism, in the present eutectic it can be inferred that ACN, with its high melting temperature, nucleates first followed by the nucleation of SCN. Thus, the phases grow by the alternate nucleation mechanism.

Thermochemistry

The phase transformation involves two steps: (i) nucleation and (ii) growth. The nucleation mechanism depends on the solid–liquid interfacial energy, which can be calculated from the heats of fusion data. However, the growth step depends on the manner in which particles from the liquid phase are added at the solid–liquid interface, which is determined by the structure of the interface. The interface structure depends on the entropy of fusion of the material under investigation and also upon the thermal environment in which the crystal is growing. Thus, the heats of fusion of the pure components, eutectic and monotectic are very important in understanding the mechanism of solidification. From the heats of fusion data the entropy of fusion, interfacial energy, radius of critical nucleus, enthalpy of mixing and excess thermodynamic functions can be calculated to throw light on the behaviour of solidification and the nature of interactions between the components forming the eutectic melt.

Heat of fusion of the eutectic

The values of enthalpy of fusion of the pure components and the eutectic, determined experimentally, are reported in Table 2. If a eutectic is a simple mechanical mixture of the two components, involving no heat of mixing or

TABLE 2

Heat of fusion and entropy of fusion

Material	Heat of fusion ($kJ\ mol^{-1}$)	Entropy of fusion ($J\ K^{-1}\ mol^{-1}$)
Acenaphthene	21.5	58.7
Succinonitrile	3.9	12.0
ACN–SCN eutectic (experimental)	3.1	9.6
ACN–SCN eutectic (by mixture law)	4.1	12.7

any type of association in the melt, the heat of fusion may simply be given by the mixture law [26]

$$(\Delta_f h)_e = x_1 \Delta_f h_1^\circ + x_2 \Delta_f h_2^\circ \tag{2}$$

where x and $\Delta_f h^\circ$ are the mole fraction and heat of fusion respectively, of the component indicated by the subscript. For the purpose of comparison, the calculated value is also given in the same table. When a solid eutectic melts, there is a considerable possibility of association and heat of mixing, both causing violation of the mixture law. Besides the heat of mixing, another factor, i.e. the interfacial energy σ_{L-S} may also affect the magnitude of the heat of fusion value. If this is so, the heat of fusion may be represented as the sum of the following forms

$$(\Delta_f h)_e = x_1 \Delta_f h_1^\circ + x_2 \Delta_f h_2^\circ + \Delta H_m + \sigma_{L-S} A \tag{3}$$

where ΔH_m and A represent the heat of mixing and the surface area, respectively.

The heat of mixing ΔH_m [27], which is the difference between the experimental and the calculated values of heats of fusion, is found to be -1.0 kJ mol^{-1}. Thermochemical studies suggest that the structure of a binary eutectic melt depends on the sign and magnitude of the heat of mixing. As such, three types of structures are suggested, (i) quasieutectic, for which $\Delta H_m > 0$, (ii) clustering of molecules, in which case $\Delta H_m < 0$, and (iii) molecular solutions, for which $\Delta H_m = 0$. The negative value of ΔH_m for the eutectic under investigation suggests clustering of molecules in the binary melt.

Entropy of fusion and excess thermodynamic functions

The entropy of fusion gives an idea as to the role of this factor in the melting of the eutectic. The excess thermodynamic functions provide a quantitative measure of the deviation of the system from ideal behaviour. Theoretical studies on the entropy of fusion and the calculation of excess thermodynamic functions of the eutectic also predict the structure, stability and ordering in the eutectic melt. The entropy of fusion ($\Delta_f S$) was calculated from the following equation

$$\Delta_f S = \frac{\Delta_f h}{T} \tag{4}$$

where $\Delta_f h$ is the heat of fusion and T is the melting temperature. The calculated values of entropy of fusion, reported in Table 2, are all positive and from these it can be inferred that both factors, namely energy and entropy, favour the melting process of the components and the eutectic.

With a view to understanding the nature of interaction between the components forming the eutectic, some excess thermodynamic functions, such as free energy (g^E), enthalpy (h^E) and entropy (s^E), were computed.

TABLE 3

Excess thermodynamic functions for the eutectic

Function	Value ($J\ mol^{-1}$)
g^E	70.6
h^E	580.2
s^E	1.6

Using the eutectic temperature and composition, the excess thermodynamic functions were calculated [26] from the following equations

$$g^E = RT(x_1 \ln \gamma_1^l + x_2 \ln \gamma_2^l) \tag{5}$$

$$h^E = -RT^2\left(x_1 \frac{\delta \ln \gamma_1^l}{\delta T} + x_2 \frac{\delta \ln \gamma_2^l}{\delta T}\right) \tag{6}$$

$$s^E = -R\left(x_1 \ln \gamma_1^l + x_2 \ln \gamma_2^l + x_1 T \frac{\delta \ln \gamma_1^l}{\delta T} + x_2 T \frac{\delta \ln \gamma_2^l}{\delta T}\right) \tag{7}$$

The activity coefficient, γ_i^l, of component i in the liquid phase in the system was calculated by

$$-\ln x_i^l \gamma_i^l = \frac{\Delta_f h_i^\circ}{R}\left(T^{-1} - T_i^{\circ -1}\right) \tag{8}$$

where x_i^l, $\Delta_f h_i^\circ$ and T_i° are the mole fraction, heat of fusion and melting temperature of component i, respectively; R is the gas constant and T is the melting temperature of the eutectic. The value of $\delta \ln \gamma_i^l / \delta T$ can be determined by the liquidus curve of the phase diagram. The computed values of the excess thermodynamic functions are reported in Table 3. It is evident from the table that the values of all excess thermodynamic functions are positive. The positive value of g^E predicts [28] that molecular association between like molecules is stronger than between unlike molecules. The value of excess entropy measures the change in configurational energy due to change in potential energy, and it indicates an increase in randomness.

Interfacial energy

The magnitude of the heat of fusion is affected by the interfacial tension. The solid–liquid interface plays an important role in determining the kinetics of phase transformation. During the growth of a crystal the radius of the critical nucleus is influenced by undercooling as well as the interfacial energy of the surface involved. The interfacial energy (σ) is given by the expression [29]

$$\sigma = \frac{C\Delta_f H}{N^{1/3}(V_m)^{2/3}} \tag{9}$$

TABLE 4

Interfacial energies in ACN–SCN system

Parameter	Value (erg cm^{-2})
$\sigma_{SL_2(SCN)}$	8.18
$\sigma_{SL_1(ACN)}$	29.73
$\sigma_{L_1L_2(ACN-SCN)}$	6.72
$\sigma_{E(ACN-SCN)}$	8.40

where N is the Avogadro number, V_m is the molar volume and parameter C lies between 0.30 and 0.35. The calculated values of the interfacial energy for different materials are reported in Table 4. Recently, articles [30,31] have been published which explain various interesting phenomena which occur during the solidification of a monotectic alloy. In particular, the role of wetting in a phase-separation process is of immense importance in the present context. The wetting condition is given as

$$\sigma_{SL_2} < \sigma_{SL_1} + \sigma_{L_1L_2}$$

where σ is the interfacial energy between the faces denoted by the subscripts. The value of $\sigma_{L_1L_2}$ was calculated using the following equation [32]

$$\sigma_{L_1L_2} = \sigma_{SL_1} + \sigma_{SL_2} - 2\sqrt{\sigma_{SL_1}\sigma_{SL_2}} \tag{10}$$

To check the validity of the Cahn wetting condition and to predict the mode of solidification morphology in the present system, the interfacial energies were calculated at the monotectic temperature, and the results are given in Table 4. It is evident from the numerical values of the interfacial energies that the Cahn wetting condition is applicable in the present system.

Radius of critical nucleus

It is well known that the melt contains a number of tiny particles, each containing a large number of molecules. If the size of a particle is smaller than the size of the critical nucleus, it is called an embryo, and it does not provide a stable nucleus for subsequent growth to take place. When the particle size corresponds to the size of the critical nucleus, it gives a stable nucleus for the growth of the crystal. The radius of the critical nucleus (r^*) depends on the interfacial energy, the melting temperature (T) and the undercooling (ΔT) according to the following equation [33]

$$r^* = \frac{2\sigma T}{\Delta H_f \Delta T} \tag{11}$$

where ΔH_f is the enthalpy of fusion per unit volume. The radius of the critical nucleus was calculated at different undercoolings, and the results are reported in Table 5. It is evident from the table that the radius of the critical nucleus decreases with increase in the undercooling of the melt. According

TABLE 5

Radius of critical nucleus at different degrees of undercooling

Undercooling (ΔT °C)	Critical radius $\times 10^6$ (cm)		
	ACN	SCN	Eutectic
2.0	7.63		
2.5		4.43	
3.0	5.09	3.69	
3.5		3.16	4.09
4.0	3.82	2.77	3.58
4.5		2.46	3.18
5.0	3.05		2.86
5.5			2.60
6.0			2.38
6.5			2.20

to eqn. (11) one can estimate the size of embryo required to form a critical nucleus at any temperature. This does not tell us whether an embryo of that size actually exists in the liquid at that temperature. However, by intuition one can expect a range of embryo sizes in the liquid at any temperature. It can be anticipated that the higher the temperature, the smaller the largest size of embryo, due to the increased amplitude of atomic vibrations at the higher temperature.

Microstructure

The microstructure gives the shape, size and distribution of grains, and these factors control the mechanical properties of the materials. The shape [33] that a crystal adopts in the melt subsequent to nucleation is controlled by the way in which molecules are added on to the solid, which in turn is determined by the atomic structure of the growing interface. Depending on the entropy of fusion of a material, the growing interface may be either rough and non-crystalline in character or atomically smooth and crystalline. The undercooling of the interface provides the driving force of the kinetic process in the direction of freezing, and its magnitude decides the rate of growth. Although the growth rate is dependent only on the interface temperature, the actual form that develops depends on the thermal condition ahead of the interface. While the solid–liquid interface of an organic analogue of a metal propagates normal to itself by the direct addition of molecules everywhere over the surface, an organic analogue of a non-metal grows by the lateral migration of growth steps across the surface. In the case of a eutectic, where a liquid phase gives two solid phases, and a monotectic, in which a liquid provides a liquid and a solid phase, the situation becomes even more complicated owing to rejection of solute and its subsequent diffusion towards the respective phases.

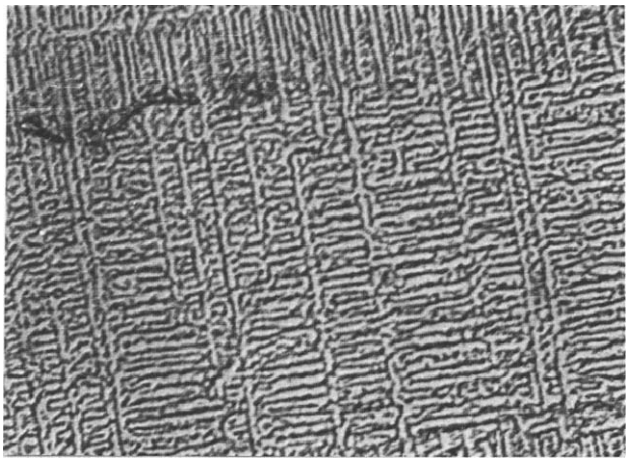

Fig. 3. Microstructure of ACN–SCN eutectic (original magnification, ×600).

Microstructure of the eutectic

In the eutectic reaction a liquid phase dissociates into two solid phases. The two solid phases solidify side-by-side: the factors which determine their growth pattern are the direction of heat flow and the interdiffusion of the two components in the liquid phase, plus, to a minor extent, the crystalline orientation relationship between the phases. In the present system, ACN, with its high entropy of fusion, will tend to solidify in a faceted and crystalline fashion and the second component SCN, with its low entropy of fusion, will solidify in a non-faceted and non-crystalline pattern. As each phase grows into the liquid it rejects a given amount of the other component, which has to diffuse away across the interface to be taken up by the growth of the other phase. The microstructure of the ACN–SCN eutectic is shown in Fig. 3 in the form of cellular dendrites. This morphology is obtained because of the cellular interface resulting from a negative temperature gradient in the liquid ahead of the interface. A large constitutional supercooling due to a shallow temperature gradient at the solid–liquid interface is also responsible for the cellular dendritic microstructure.

Microstructure of the monotectic

The microstructure of the ACN–SCN monotectic, given in Fig. 4, shows a well arranged array of droplets. When (ACN–SCN) liquid (L_1) is allowed to cool below the monotectic temperature (T_M), solid ACN deposits. The liquid adjacent to the interface solid (ACN–L_1) is enriched with SCN owing to solute rejection and it therefore becomes supersaturated with respect to SCN; droplets of SCN (L_2) then nucleate to relieve the supersaturation. Whether the liquid L_2 droplets nucleate in the melt or on the solid–liquid interface depends upon the relative magnitudes of the three interfacial energies, namely, σ_{SL_1}, σ_{SL_2} and $\sigma_{L_1L_2}$. It is evident from the data reported in

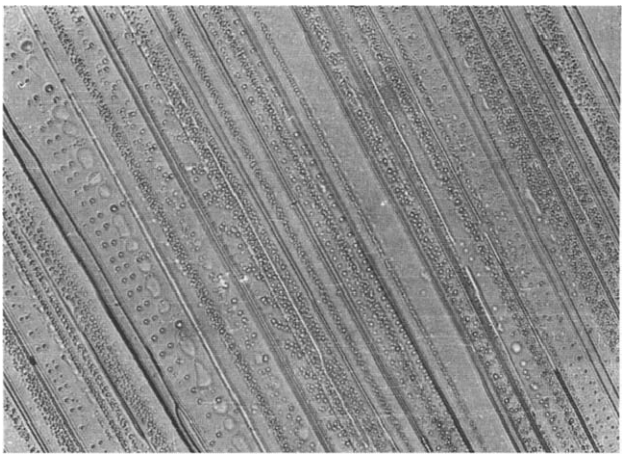

Fig. 4. Microstructure of $\overline{ACN}$–SCN monotectic (original magnification, ×600).

Table 4 that the Cahn wetting condition can be successfully applied to the present system. Accordingly, the interfacial energies are related by

$$\sigma_{SL_2} < \sigma_{SL_1} + \sigma_{L_1L_2}$$

Thus the ACN–SCN liquid (L_1) wets the solidified ACN perfectly, and SCN-rich droplets (L_2) will be surrounded by (ACN–SCN) liquid. Under this situation, there is the possibility of capillary instabilities of the type observed in the Al–Bi system [11,34]. If the cell depths are greater than the droplet circumference, capillary instabilities will develop SCN droplets and they will pinch off into spheres. ACN-rich liquid subsequently solidifies behind these spheres. Repetition of this process produces a very well arranged array of spheres, as observed in Fig. 4.

ACKNOWLEDGEMENT

Thanks are due to Prof. P. Chandra, Head of the Chemistry Department, Banaras Hindu University for providing research facilities.

REFERENCES

1 R. Grugel and W. Kurz, Metall. Trans., A, 18 (1987) 1137.
2 R. Elliott, Int. Met. Rev., 22 (1977) 161.
3 R.G. Pirich, Metall. Trans., A, 15 (1984) 2139.
4 S. Chaubey, V. Singh and P.R. Rao, Trans. Indian Inst. Met., 41 (1988) 147.
5 C.C. Coch, Int. Mater. Rev., 33 (1988) 201.
6 R.N. Grugel and A. Hellawell, Metall. Trans., A, 15 (1984) 1626.
7 M.E. Glicksman, N.B. Singh and M. Chopra, Manuf. Space, 11 (1983) 207.
8 R.P. Rastogi, D.P. Singh, N. Singh and Narsingh B. Singh, Mol. Cryst. Liq. Cryst., 73 (1981) 7.
9 J.D. Hunt and K.A. Jackson, Trans. Metall. Soc. AIME, 236 (1966) 843.

10 W.F. Kaukler and D.O. Frazier, J. Cryst. Growth, 71 (1985) 340.
11 N.B. Singh, U.S. Rai and O.P. Singh, J. Cryst. Growth, 71 (1985) 353.
12 S.-Y.OH, J.A. Cornie and K.D. Russell, Metall. Trans., A, 20 (1989) 527.
13 Narsingh B. Singh, Sci. Rep., 24 (1987) 212.
14 R.N. Grugel and A. Hellawell, Metall. Trans., A, 12 (1981) 669.
15 U.S. Rai, O.P. Singh and Narsingh B. Singh, J. Chim. Phys., 84 (1987) 483.
16 R.P. Rastogi and V.K. Rastogi, J. Cryst. Growth, 5 (1969) 345.
17 U.S. Rai and K.D. Mandal, Bull. Chem. Soc. Jpn., 63 (1990) 1496.
18 N.B. Singh and Narsingh B. Singh, Krist. Tech., 13 (1978) 1175.
19 U.S. Rai and K.D. Mandal, Can. J. Chem., 67 (1989) 239.
20 J.W. Dodd and K.H. Tonge, in B.R. Currell (Ed.), Thermal Methods (Analytical Chemistry by Open Learning Series), Wiley, Chichester, 1987, p. 120.
21 R.P. Rastogi, N.B. Singh and Narsingh B. Singh, J. Cryst. Growth, 37 (1977) 329.
22 U.S. Rai and K.D. Mandal, Mol. Cryst. Liq. Cryst. B, 182 (1990) 387.
23 D. Derby and J.J. Favier, Acta Metall., 31 (1983) 1123.
24 W.B. Hillig and D. Turnbull, J. Chem. Phys., 24 (1956) 914.
25 W.C. Winegard, S. Mojka, B.M. Thall and B. Chalmers, Can. J. Chem., 29 (1957) 320.
26 U.S. Rai, K.D. Mandal and N.P. Singh, J. Therm. Anal., 35 (1989) 1687.
27 U.S. Rai, O.P. Singh and Narsingh B. Singh, Can. J. Chem., 65 (1987) 2639.
28 R.A. Swalin, Thermodynamics of Solids, Wiley, New York, 1972, p. 136.
29 Narsingh B. Singh, Acta Cienc. Indica, 4 (1978) 4.
30 R.N. Grugel, T.A. Lograsso and A. Hellawell, Metall. Trans., A, 15 (1984) 1003.
31 J.W. Cahn, Metall. Trans., A, 10 (1979) 119.
32 R. Good, Ind. Eng. Chem., 62 (1970) 54.
33 G.A. Chadwick, Metallography of Phase Transformation, Butterworth, 1972, pp. 86–158.
34 C. Schafer, M.H. Johnston and R.A. Parr, Acta Metall., 31 (1983) 1221.